Available online at www.worldscientificnews.com

World Scientific News

WSN 88(2) (2017) 138-151 EISSN 2392-2192

A DFT study or the relationship between the electronic structure and the antiplasmodial activity of a series of 4-anilino-2-trichloromethylquinazolines derivatives

Wilfried Anatovi[1], Gaston A. Kpotin[1,*], Urbain A. Kuevi[1], Alice Houngue-Kpota[1], Guy S. Atohoun[1], Jean-Baptiste Mensah[1] and **Juan S. Gómez-Jeria[2]**

[1]Laboratory of Theoretical Chemistry and Molecular Spectroscopy,
Faculty of Sciences and Techniques, University of Abomey - Calavi, 03 BP 3409 Cotonou, Benin

[2]Quantum Pharmacology Unit, Department of Chemistry, Faculty of Science, University of Chile,
Las Palmeras 3425, Nuñoa, Santiago 7800003, Santiago, Chile

*E-mail adddress: gaston.kpotin@fast.uac.bj

ABSTRACT

A theoretical study of the relationships between the electronic structure and the antiplasmodial activity of a series of 4-anilino-2-trichloromethylquinazolines derivatives on plasmodium genes was carried out. The electronic structure of molecules was calculated at the B3LYP/6-31G(d,p) level with full geometry optimization. A statistically significant equation ($R = 0.98$, $R^2 = 0.96$, adj-$R^2 = 0.94$, $F(12, 20) = 43.49$ ($p < 0.000001$) and $SD = 0.12$) was obtained relating the variation of the biological activity with the variation of a set of local atomic reactivity indices. Based on the analysis of the results, a two-dimensional antiplasmodial pharmacophore was proposed. The process seems to be orbital and charge controlled.

***Keywords*:** antiplasmodial, DFT, QSAR, KPG method, 4-anilino-2-trichloromethylquinazolines

1. INTRODUCTION

Malaria is one of the most devastating diseases in the third-world countries. Malaria is caused by parasites of the genus *Plasmodium* [1]. The infections caused by *Plasmodium falciparum* is prevalent in the major parts of Africa, sub-Saharan Africa and East Asian countries [2].

The global tally of malaria in 2015 was 212 million new cases and 429 000 deaths. Across Africa, millions of people still lack access to the tools they need to prevent and treat the disease. Funding shortfalls and fragile health systems restrict access to life-saving interventions and jeopardize the attainment of global targets. According to the report, fewer than half of the 91 malaria-affected countries and territories are on track to achieve the 2020 milestone of a 40% reduction in case incidence and mortality [3].

Vaccines developed are of limited efficacy [4–6]. The hybrid vaccine *RTS,S/AS01* still in the experimental phase, is one of the best authorized by the WHO [6–8]. Medicines used in the treatment of malaria are: Primaquine, chloroquine, quinine, mefloquine, halofantrine, lumefantrine, piperaquine, proguanil and artemisinin derivatives (artemether, artemminol, dihydroartemisin proguanil) [9].

Each of these drugs has one or more problems such as ineffectiveness against early or advanced stages, toxicity and resistances [10,11]. Recent studies have shown several biological activities of quinazolines; including their anti-malarial antiplasmodial [12–23] anti-leishmaniasis [20] and antileishmanial [24] activities. In this work we present a study on the relationship between the electronic structure and the antiplasmodial activity of a series of 4-anilino-2-trichloromethylquinazolines on malaria.

2. METHODS, MODELS AND CALCULATIONS.

2. 1. Model and Application

The technique employed to perform quantitative structure-activity relationships is the Klopman-Peradejordi-Gómez (KPG) method. Since this method has been fully discussed in previous papers, we will discuss here only the results [25–33]. From a conceptual perspective the work presented here is a test of the hypothesis stating that the KPG model can provide a quantitative and formal relationship between the molecular structure and any biological activity. In fact, it is show that $\log(IC_{50})$ is a linear function of local atomic reactivity index. Nowadays, the KPG model produced excellent results in all its applications [31–40].

For the application of this method, a series of thirty three selected molecules are derived from the quinazoline derivatives obtained based on 4-anilino-quinazolines, exhibit anti-malaria activity. The structures of these compounds are shown in figure 1. Table 1 summarize the values of their median inhibitory concentrations IC_{50}, those values were taken from literature [21].

These experimental data used in this study are the antiplasmodial activities expressed in μmol/L. The tests are performed on the blood form of Plasmodium W2 strains.

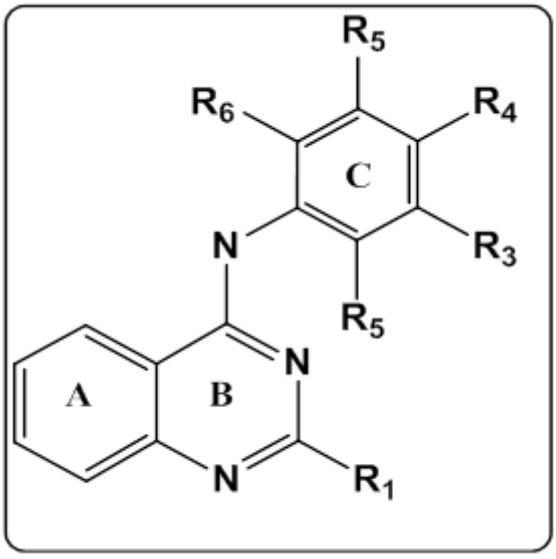

Figure 1. Structure of 4-anilino-quinazolines.

Table 1. Selected molecules and their anti-plasmodial activities.

Mol.	R_1	R_2	R_3	R_4	R_5	R_6	$\log(IC_{50})$
1	CCl_3	H	H	H	H	H	1.04
2	CCl_3	F	H	H	H	H	0.95
3	CCl_3	H	F	H	H	H	0.60
4	CCl_3	H	H	F	H	H	0.73
5	CCl_3	Cl	H	H	H	H	0.66
6	CCl_3	H	Cl	H	H	H	0.23
7	CCl_3	H	H	Cl	H	H	0.48
8	CCl_3	Br	H	H	H	H	0.48
9	CCl_3	H	Br	H	H	H	0.34
10	CCl_3	H	H	Br	H	H	0.18
11	CCl_3	CH_3	H	H	H	H	0.84
12	CCl_3	H	CH_3	H	H	H	0.36
13	CCl_3	H	H	CH_3	H	H	0.38

14	CCl_3	CF_3	H	H	H	H	0.87
15	CCl_3	H	CF_3	H	H	H	0.26
16	CCl_3	H	H	CF_3	H	H	0.20
17	CCl_3	OCH_3	H	H	H	H	0.78
18	CCl_3	H	OCH_3	H	H	H	0.60
19	CCl_3	H	H	OCH_3	H	H	0.78
20	CCl_3	NO_2	H	H	H	H	0.48
21	CCl_3	H	NO2	H	H	H	0.48
22	CCl_3	H	H	NO_2	H	H	0.45
23	CCl_3	Cl	Cl	H	H	H	1.15
24	CCl_3	Cl	H	Cl	H	H	-0.40
25	CCl_3	Cl	H	H	Cl	H	0.23
26	CCl_3	Cl	H	H	H	Cl	1.34
27	CCl_3	H	Cl	Cl	H	H	0.70
28	CCl_3	H	Cl	H	Cl	H	0.60
29	CCl_3	H	CF_3	H	CF_3	H	0.45
30	CCl_3	H	H	OCF_3	H	H	0.46
31	CH_3	H	Cl	H	H	H	1.74
32	CH_3	H	CF_3	H	H	H	1.63
33	CH_3	Cl	H	Cl	H	H	1.93

2. 2. Calculation method

The electronic structure of each optimized molecule was obtained using the Density Functional Theory (DFT) at B3LYP/6-31G (d, p) level with the Gaussian software [41]. The local reactivity indices were calculated from the Single Point results using the D-Cent-QSAR software [42] with a correction of the Mulliken population [43]. All populations of electrons less than or equal to 0.01e are considered null [43]. The orientational parameters of the substituents are calculated in the usual manner [44,45]. We have used the hypothesis of the common skeleton: It is a set of atoms common to all the molecules analyzed, which accounts for all the biological activity. The variation of the values of the set of local atomic reactivity indices of certain atoms along the skeleton should give an explanation to the variation of the

antiplasmodial activity through the series analyzed. We used the technique of multiple linear regression analysis to determine the atoms that are directly involved in the variation of biological activity. The data matrix contains the log (IC_{50}) as a dependent variable, and the local indices of atomic reactivity of all the atoms of the common skeleton as independent variables. Statistica software was used to perform multiple linear regression analysis [46]. The numbering of the common skeleton atoms is shown in Figure 2.

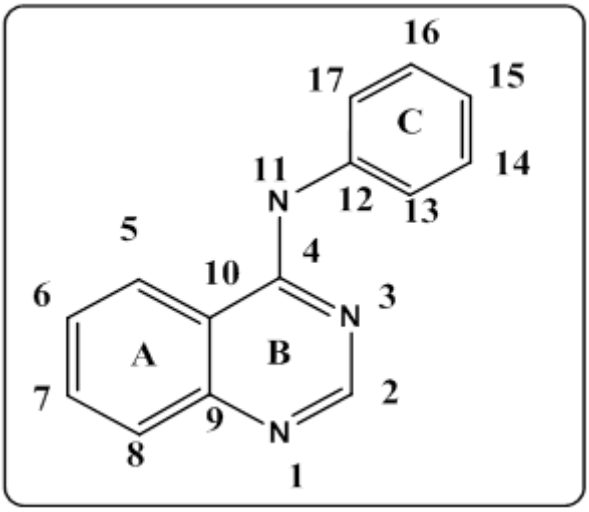

Figure 2. Common skeleton numbering.

3. RESULTS

The best statistically significant equation obtained is the following:

$$\log(IC_{50}) = -13.26 - 2S_2^E - 2.47F_{17}(HOMO-2)^* - 2.19F_{15}(HOMO)^* - 0.003S_9^N(LUMO+2)^* - 0.0005S_{13}^N + 0.001S_{13}^N(LUMO+2)^* \quad (1)$$

with n = 29, R = 0.97, R^2 = 0.94, adj-R^2 = 0.92, F (6.22) = 55.17 ($p < 0.000001$), and a standard error of the estimate of 0.14. No outliers were detected and no residuals fall outside ± 2σ limit. Here, S_2^E is the total atomic electrophilic superdelocalizability of atom 2, $F_{17}(HOMO-2)$* is the Fukui index (electron population) the third highest occupied MO localized on atom 17, $F_{15}(HOMO)$* is the Fukui index (electron population) the highest occupied MO localized on atom 15, $S_9^N(LUMO+2)$* is the nucleophilic superdelocalizability of the third lowest empty MO localized on atom 9, S_{13}^N is the total atomic nucleophilic superdelocalizability of atom 13 and $S_{13}^N(LUMO+2)$* is the nucleophilic superdelocalizability of the third lowest empty MO localized on atom 13. Tables 2 and 3 show the beta coefficients, the results of the t-test for the significance of the coefficients and the matrix of squared correlation coefficients for the variables of equation 1. There are no significant internal correlations between independent variables (Table 3). Figure 3 displays the plot of observed vs. calculated log(IC_{50}) values.

The associated statistical parameters of Eq. 1 indicate that this equation is statistically significant and that the variation of the numerical values of a group of six local atomic reactivity indices of atoms of the common skeleton explains about 92% of the variation of log(IC_{50}).

Table 2. Beta Coefficients and t-test of the coefficients in equation 1.

Variables	Beta coefficients	t(22)	p-level
S_2^E	-0.67	-11.49	0.0000001
$F_{17}(HOMO-2)^*$	-0.44	-7.79	0.0000001
$F_{15}(HOMO)^*$	-0.24	-3.63	0.001
$S_9^N(LUMO+2)^*$	-0.19	-3.31	0.003
S_{13}^N	-0.20	-3.11	0.005
$S_{13}^N(LUMO+2)^*$	0.18	2.45	0.02

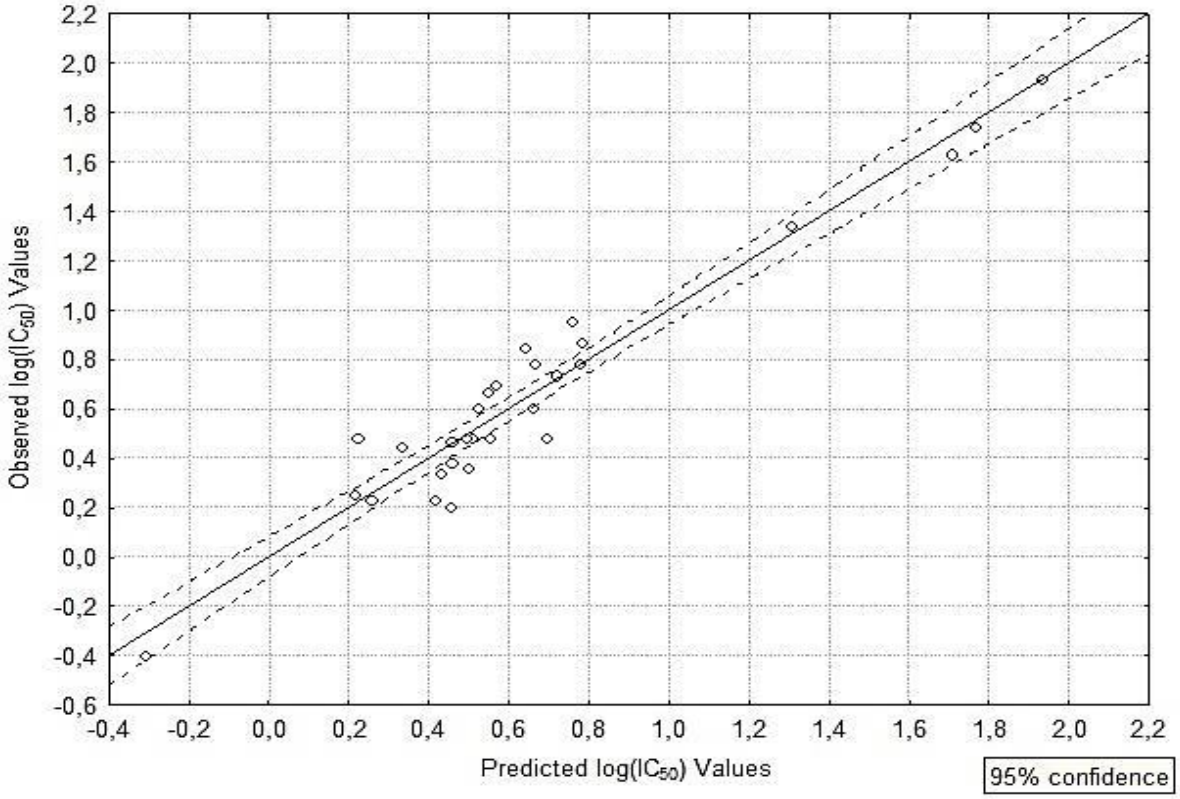

Figure 3. Plot of predicted vs. observed log(IC50) values. Dashed lines denote the 95% confidence interval

Table 3. Squared correlation coefficients for the variables of equation 1.

	S_2^E	$F_{17}(HOMO-2)^*$	$F_{15}(HOMO)^*$	$S_9^N(LUMO+2)^*$	S_{13}^N
$F_{17}(HOMO-2)^*$	0.006	1.00			
$F_{15}(HOMO)^*$	0.05	0.02	1.00		
$S_9^N(LUMO+2)^*$	0.04	0.02	0.03	1.00	
S_{13}^N	0.05	0.007	0.0002	0.00004	1.00
$S_{13}^N(LUMO+2)^*$	0.008	0.03	0.22	0.006	0.20

Tables 4 and 5 show the Local Molecular Orbitals of atoms 2, 9, 13, 15, and 17 (see Fig. 3). Nomenclature: Molecule (HOMO) / (HOMO-2)* (HOMO-1)* (HOMO)* - (LUMO)* (LUMO+1)* (LUMO+2)*.

Table 4. Local Molecular Orbitals of atoms 2, 9 and 13

.

Molecule (HOMO)	Atom 2 (C)	Atom 9 (C)	Atom 13(C)
1(86)	84π85π86π-87π88π89π	84π85π86π- 88π90π91π	83π85π86π-87π88π90π
2(90)	88π89π90π-91π92π93π	88π89π90π-92π94π95π	87π89π90π-91π94π95π
3(90)	88π89π90π-91π92π95π	88π89π90π-92π94π95π	87π89π90π-91π92π94π
4(90)	88π89π90π-91π92π93π	88π89π90π-92π95π96π	78π87π90π-91π92π94π
5(94)	92π93π94π-95π96π97π	92π93π94π- 96π99π100π	91π93π94π-95π96π98π
6(94)	92π93π94π-95π96π97π	92π93π94π- 96π99π100π	91π93π94π-95π96π98π
7(94)	92π93π94π-95π96π97π	92π93π94π-96π99π100π	88π91π94π-95π96π98π
8(103)	101π102π103π-104π105π106π	101π102π103π-105π109π110π	101π102π103π-104π105π107π
9(103)	101π102π103π-104π105π106π	101π102π103π-105π108π110π	100π102π103π-104π105π107π
10(103)	101π102π103π-104π105π106π	101π102π103π-105π108π109π	99π100π103π-104π105π107π
11(90)	87π88π90π-91π92π93π	87π88π90π-92π94π95π	88π89π90π-91π94π95π
12(90)	88π89π90π-91π92π93π	87π88π90π-92π94π96π	88π89π90π-91π94π95π
13(90)	88π89π90π-91π92π93π	88π89π90π-92π94π95π	88π89π90π-91π92π94π
14(102)	100π101π102π-103π104π106π	100π101π102π-103π104π107π	99π100π102π-103π104π105π
15(102)	100π101π102π-103π104π105π	100π101π102π-104π107π108π	99π100π102π-103π104π106π
16(102)	100π101π102π-103π104π105π	100π101π102π-103π104π106π	89π99π102π-103π104π106π
17(94)	92π93π94π-95π96π97π	92π93π94π-96π98π99π	83π93π94π-95π99π100π
18(94)	92π93π94π-95π96π97π	92π93π94π-96π98π99π	91π93π94π-95π96π98π

19(94)	91π92π93π-95π96π97π	92π93π94π-96π99π100π	91π93π94π-95π96π98π
20(97)	95π96π97π-99π100π101π	95π96π97π-100π102π103π	94π96π97π-98π102π103π
21(97)	95π96π97π-99π100π101π	95π96π97π-99π100π102π	94π95π97π-98π99π100π
22(97)	95π96π97π-98π99π100π	95π96π97π-98π99π100π	94π95π97π-98π100π102π
23(102)	99π100π102π-103π104π105π	99π100π102π-103π104π107π	100π101π102π-103π104π106π
24(102)	100π101π102π-103π104π105π	100π101π102π-103π104π107π	99π101π102π-103π104π106π
25(102)	100π101π102π-103π104π105π	100π101π102π-103π104π107π	96π101π102π-103π104π106π
26(102)	100π101π102π-103π104π107π	100π101π102π-104π109π113π	100π101π102π-103π105π106π
27(102)	100π101π102π-103π104π105π	100π101π102π-103π104π107π	99π101π102π-103π104π106π
28(102)	99π100π102π-103π104π105π	99π100π102π-103π104π107π	100π101π102π-103π104π106π
29(118)	116π117π118π-119π120π121π	116π117π118π-119π120π121π	115π116π118π-119π120π121π
30(106)	104π105π106π-107π108π109π	104π105π106π-108π111π112π	95π103π106π-107π108π110π
31(70)	68π69π70π-71π72π76π	68π69π70π-71π72π73π	67π69π70π-71π72π73π
32(78)	76π77π78π-79π80π81π	76π77π78π-79π80π81π	75π76π78π-79π80π81π
33(78)	76π77π78π-79π80π81π	76π77π78π-79π80π81π	75π77π78π-79π80π81π

Table 5. Local Molecular Orbitals of atoms 15 and 17.

Molecule (HOMO)	Atom 15(C)	Atom 17(C)
1(86)	83π85π86π- 87π88π90π	84π85π86π- 87π90π91π
2(90)	87π89π90π-91π92π94π	88π89π90π-91π94π95π
3(90)	87π89π90π-91π92π94π	88π89π90π-91π94π95π
4(90)	84π89π90π-91π94π95π	88π89π90π-91π94π95π
5(94)	91π93π94π- 95π96π98π	92π93π94π- 95π98π99π
6(94)	91π93π94π-95π96π98π	92π93π94π-95π98π99π
7(94)	88π93π94π-95π96π98π	92π93π94π-95π98π99π
8(103)	101π102π103π-104π105π107π	101π102π103π-104π107π108π
9(103)	100π102π103π-104π105π107π	101π102π103π-104π107π108π
10(103)	98π102π103π-104π105π107π	101π102π103π-104π107π108π
11(90)	86π88π90π-91π94π95π	88π89π90π-91π94π95π
12(90)	88π89π90π-91π92π94π	88π89π90π-91π94π95π
13(90)	88π89π90π-91π94π95π	88π89π90π-91π94π95π
14(102)	100π101π102π-103π104π105π	100π101π102π-103π105π107π
15(102)	99π100π102π-103π104π106π	100π101π102π-103π106π107π
16(102)	99π100π102π-103π104π106π	100π101π102π-103π106π107π

17(94)	90π92π94π-95π96π98π	92π93π94π-95π98π99π
18(94)	90π91π94π-95π96π98π	92π93π94π-95π98π99π
19(94)	91π93π94π-95π98π99π	92π93π94π-95π98π99π
20(97)	94π96π97π-99π100π102π	95π96π97π-98π99π100π
21(97)	94π95π97π-98π99π100π	95π96π97π-98π102π103π
22(97)	94π95π97π-98π102π103π	95π96π97π-98π102π103π
23(102)	100π101π102π-103π104π106π	99π101π102π-103π106π107π
24(102)	99π101π102π-103π104π106π	99π100π102π-103π106π107π
25(102)	99π101π102π-103π104π106π	100π101π102π-103π106π107π
26(102)	99π101π102π-103π104π105π	100π10π1102π-103π104π105π
27(102)	99π101π102π-103π104π106π	100π101π102π-103π106π107π
28(102)	98π100π102π-103π104π106π	100π101π102π-103π106π107π
29(118)	115π116π118π-119π120π121π	116π117π 118π-119π121π123π
30(106)	103π105π106π-107π108π110π	104π105π106π-107π110π111π
31(70)	67π69π70π-71π73π74π	68π69π70π-71π72π73π
32(78)	75π76π78π-79π81π82π	76π77π78π-79π80π81π
33(78)	74π77π78π-79π81π82π	76π77π78π-79π80π81π

4. DISCUSSION

The results obtained indicate that the variation of the antiplasmodial activity of these quinazolines derivatives is related to the variation of the numerical values of a set of six local atomic reactivity indices of the common skeleton. This result is very good considering the approximations made to construct the model.

The beta values shows that the importance of variables is $S_2^E > F_{17}(HOMO-2)^* > F_{15}(HOMO)^* > S_{13}^N \approx S_9^N(LUMO+2)^* \approx S_{13}^N(LUMO+2)^*$. The process seems to be orbital-controlled. A variable-by-variable analysis indicates that a good activity is associated with low negative numerical values of S_2^E (they are always negative), with high numerical values of $F_{17}(HOMO-2)^*$ and $F_{15}(HOMO)^*$ (their values are always positive). If S_{13}^N is positive, a high inhibitory activity is associated with high numerical values.

If $S_9^N(LUMO+2)^*$ is positive, a good activity is associated with high numerical values for this index. If $S_{13}^N(LUMO+2)^*$ is positive, a high inhibitory activity is associated with low numerical values. Atom 2 is a carbon in ring A (Fig. 2). Table 4 shows that all local MOs have π nature. A low value of S_2^E indicates that atom 2 should interact with a π electron rich center through its empty π local MOs. Atom 17 is a carbon in ring C (Fig. 2). Table 5 shows that all local MOs have a π nature. A high value of $F_{17}(HOMO-2)^*$ suggests that atom 17 interacts with an electron-deficient center such as a cation or an aromatic moiety (a π-π interaction).

The three highest occupied local MOs participate in the modulation of the activity. Atom 15 is a carbon in ring C (Fig. 2). Table 5 shows that all local MOs have a π nature. Following a similar reasoning used for atom 17, we suggest that atom 15 is interacting with an electron-deficient center via its highest occupied local MO. Atom 13 is a carbon atom in ring C (Fig. 2). Table 4 shows that all local MOs have a π nature. If $S_9^N(LUMO+2)^*$ is positive, a higher activity is associated with higher numerical values for this index. Now, higher positive values are obtained by shifting downwards the (LUMO+2)* eigenvalue, making this MO more reactive.

Therefore, it is suggested that atom 13 is interacting with a π electron-rich center. This is confirmed by the appearance of S_{13}^N in Eq. 1 when we notice that large positive values for S_{13}^N are obtained by the same mechanism used for (LUMO+2)*. Atom 9 is a carbon atom belonging to rings A and B (Fig. 2). High numerical values of $S_9^N(LUMO+2)^*$ are associated with high activity. These values are obtained by lowering the lowest MOs eigenvalues and making these MOs more reactive. So, atom 9 should interact with a π electron-rich center. All the above suggestions are shown in the partial 2D pharmacophore (Fig. 4).

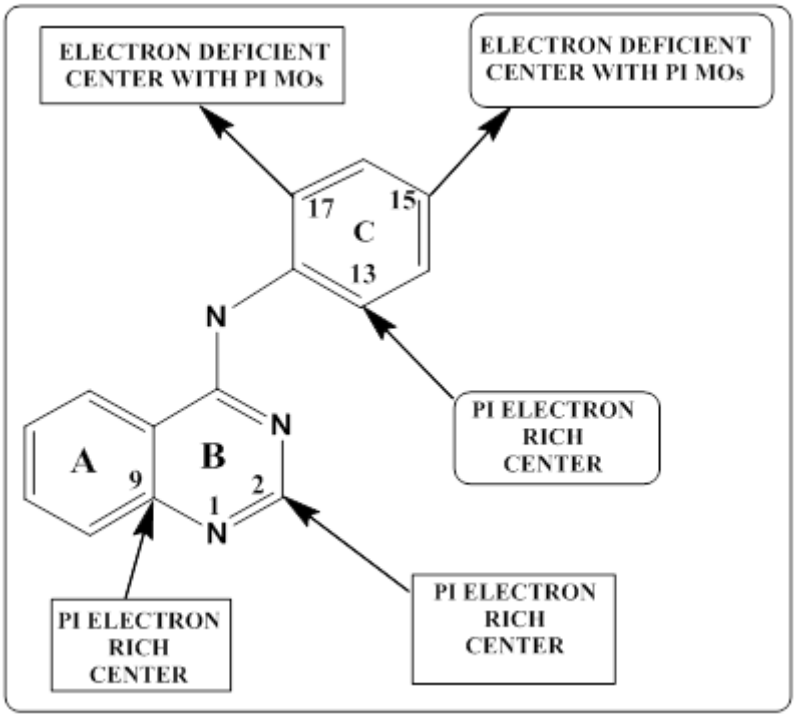

Figure 4. Proposed 2D-pharmacophore for the antiplasmodial activity of quinazoline derivatives.

4. CONCLUSION

We obtained statistically good results that show a relationship between the variation of the antiplasmodial activity and the variation of the numerical values of a set of local atomic reactivity indices. This regression equation obtained could serve as a tool for predicting the

antiplasmodial activity of quinazolines on malaria. The results were employed to build a partial two-dimensional pharmacophore. Our results could be used to make proposals for molecules with potentially stronger antiplasmodial activity.

References

[1] E.A. Ashley, J. Recht, N.J. White, Primaquine: the risks and the benefits, *Malar. J.*, 13 (2014) 418.

[2] M. Mishra, V.K. Mishra, V. Kashaw, A.K. Iyer, S.K. Kashaw, Comprehensive review on various strategies for antimalarial drug discovery, *Eur. J. Med. Chem.*, 125 (2017) 1300–1320.

[3] World Malaria Report 2016: Summary, Geneva, 2017.

[4] A.L. Wilson, on behalf of the Ipt. Taskforce, A Systematic Review and Meta-Analysis of the Efficacy and Safety of Intermittent Preventive Treatment of Malaria in Children (IPTc), *PLOS ONE*, 6 (2011) 1–12.

[5] M.M. Meremikwu, S. Donegan, D. Sinclair, E. Esu, C. Oringanje, Intermittent preventive treatment for malaria in children living in areas with seasonal transmission, *Cochrane Database Syst. Rev.*, 2 (2012).

[6] Guidelines on the Quality, Safety and Effectiveness of Recombinant Malaria Vaccines Targeting the Pre-erythrocytic and Blood Forms of Plasmodium falciparum, 2016. http://www.who.int/biologicals/vaccines/Malaria_Guidelines_TRS_980_Annex_3.pdf

[7] V.S. Moorthy, W.R. Ballou, Immunological mechanisms underlying protection mediated by RTS,S: a review of the available data, *Malar. J.*, 8 (2009) 312.

[8] A. Leach, J. Vekemans, M. Lievens, O. Ofori-Anyinam, C. Cahill, S. Owusu-Agyei, S. Abdulla, E. Macete, P. Njuguna, B. Savarese, C. Loucq, W.R. Ballou, Design of a phase III multicenter trial to evaluate the efficacy of the RTS,S/AS01 malaria vaccine in children across diverse transmission settings in Africa, *Malar. J.*, 10 (2011) 224.

[9] B. Portet, Recherche bioguidée de molecules antipaludiques d'une plante guyanaise Piper hostmannianum var berbicense, Université Toulouse III - Paul Sabatier, 2007.

[10] L. Tilley, J. Straimer, N.F. Gnädig, S.A. Ralph, D.A. Fidock, Artemisinin Action and Resistance in Plasmodium falciparum, *Trends Parasitol.*, 32 (2016) 682–696.

[11] P. Olliaro, Mode of action and mechanisms of resistance for antimalarial drugs, *Pharmacol. Ther.*, 89 (2001) 207–219.

[12] P. Verhaeghe, A. Dumètre, C. Castera-Ducros, S. Hutter, M. Laget, C. Fersing, M. Prieri, J. Yzombard, F. Sifredi, S. Rault, P. Rathelot, P. Vanelle, N. Azas, 4-Thiophenoxy-2-trichloromethyquinazolines display in vitro selective antiplasmodial activity against the human malaria parasite Plasmodium falciparum, *Bioorg. Med. Chem. Lett.*, 21 (2011) 6003–6006.

[13] A. Shrivastava, A. Shrivastava, 2D-QSAR Studies of Novel Quinazoline Derivatives for Their Potent Antimalarial Activity, *Int. J. Chem. Pharm. Rev. Res.*, 2 (2015) 1–10.

[14] C. Mendoza-Martínez, J. Correa-Basurto, R. Nieto-Meneses, A. Márquez-Navarro, R. Aguilar-Suárez, M.D. Montero-Cortes, B. Nogueda-Torres, E. Suárez-Contreras, N. Galindo-Sevilla, Á. Rojas-Rojas, A. Rodriguez-Lezama, F. Hernández-Luis, Design, synthesis and biological evaluation of quinazoline derivatives as anti-trypanosomatid and anti-plasmodial agents, *Eur. J. Med. Chem.,* 96 (2015) 296–307.

[15] J. Desroches, C. Kieffer, N. Primas, S. Hutter, A. Gellis, H. El-Kashef, P. Rathelot, P. Verhaeghe, N. Azas, P. Vanelle, Discovery of new hit-molecules targeting Plasmodium falciparum through a global SAR study of the 4-substituted-2-trichloromethylquinazoline antiplasmodial scaffold, *Eur. J. Med. Chem.,* 125 (2017) 68–86.

[16] A. Gellis, N. Primas, S. Hutter, G. Lanzada, V. Remusat, P. Verhaeghe, P. Vanelle, N. Azas, Looking for new antiplasmodial quinazolines: DMAP-catalyzed synthesis of 4-benzyloxy- and 4-aryloxy-2-trichloromethylquinazolines and their in vitro evaluation toward Plasmodium falciparum, *Eur. J. Med. Chem.,* 119 (2016) 34–44.

[17] Y. Kabri, N. Azas, A. Dumètre, S. Hutter, M. Laget, P. Verhaeghe, A. Gellis, P. Vanelle, Original quinazoline derivatives displaying antiplasmodial properties, *Eur. J. Med. Chem.,* 45 (2010) 616–622.

[18] A. Mishra, K. Srivastava, R. Tripathi, S.K. Puri, S. Batra, Search for new pharmacophores for antimalarial activity Part III: Synthesis and bioevaluation of new 6-thioureido-4-anilinoquinazolines, *Eur. J. Med. Chem.,* 44 (2009) 4404–4412.

[19] M.K. Kathiravan, N. Vidyasagar, R. Khiste, A. Chote, K. Jain, Synthesis and antihyperlipidemic activity of some novel 4-substituted-2-substitutedmethyltriazino[6,1-b]quinazolin-10-ones and 2,4-disubstituted-6,7-dimethoxy quinazoline, *Arab. J. Chem.,* 9 (2016) S395–S403.

[20] P. Verhaeghe, N. Azas, M. Gasquet, S. Hutter, C. Ducros, M. Laget, S. Rault, P. Rathelot, P. Vanelle, Synthesis and antiplasmodial activity of new 4-aryl-2-trichloromethylquinazolines, *Bioorg. Med. Chem. Lett.,* 18 (2008) 396–401.

[21] P. Verhaeghe, N. Azas, S. Hutter, C. Castera-Ducros, M. Laget, A. Dumètre, M. Gasquet, J.-P. Reboul, S. Rault, P. Rathelot, P. Vanelle, Synthesis and in vitro antiplasmodial evaluation of 4-anilino-2-trichloromethylquinazolines, *Bioorg. Med. Chem.,* 17 (2009) 4313–4322.

[22] S. Madhavi, R. Sreenivasulu, J.P. Yazala, R.R. Raju, Synthesis of chalcone incorporated quinazoline derivatives as anticancer agents, *Saudi Pharm. J.,* 25 (2017) 275–279.

[23] T. Fröhlich, C. Reiter, M.M. Ibrahim, J. Beutel, C. Hutterer, I. Zeitträger, H. Bahsi, M. Leidenberger, O. Friedrich, B. Kappes, T. Efferth, M. Marschall, S.B. Tsogoeva, Synthesis of Novel Hybrids of Quinazoline and Artemisinin with High Activities against Plasmodium falciparum, Human Cytomegalovirus, and Leukemia Cells, *ACS Omega,* 2 (2017) 2422–2431.

[24] C. Mendoza-Martínez, N. Galindo-Sevilla, J. Correa-Basurto, V.M. Ugalde-Saldivar, R.G. Rodríguez-Delgado, J. Hernández-Pineda, C. Padierna-Mota, M. Flores-Alamo, F. Hernández-Luis, Antileishmanial activity of quinazoline derivatives: Synthesis, docking

screens, molecular dynamic simulations and electrochemical studies, *Eur. J. Med. Chem.*, 92 (2015) 314–331.

[25] J.S. Gómez-Jeria, 45 Years of the KPG Method: A Tribute to Federico Peradejordi, *J. Comput. Methods Mol. Des.*, 7 (2017) 17–37.

[26] J.S. Gómez Jeria, La Pharmacologie Quantique, *Boll Chim Farm.*, 121 (1982) 619–625.

[27] J.S. Gomez-Jeria, On some problems in quantum pharmacology I The partition functions, *Int. J. Quantum Chem.*, 23 (1983) 1969–1972.

[28] J.S. Gómez Jeria, The use of competitive ligand binding results in QSAR studies, Il Farm., 40 (n.d.) 299–302.

[29] J.S. Gómez-Jeria, Modeling the Drug-Receptor Interaction in Quantum Pharmacology, in: J. Maruani (Ed.), Mol. Phys. Chem. Biol., Springer Netherlands, Dordrecht, 1989: pp. 215–231.

[30] J.S. Gómez Jeria, Elements of Molecular Electronic Pharmacology, 1st ed., Ediciones Sokar, Santiago de Chile, 2013.

[31] J.S. Gómez Jeria, A new set of local reactivity indices within the Hartree-Fock-Roothaan and density functional theory frameworks, *Can. Chem. Trans.*, 1 (2013) 25–55.

[32] J.S. Gómez Jeria, M. Flores-Catalán, Quantum-chemical Modeling of the Relationships between Molecular Structure and In Vitro Multi-Step, Multimechanistic Drug Effects HIV-1 Replication Inhibition and Inhibition of Cell Proliferation as Examples, *Can. Chem. Trans.*, 1 (2013) 215–237.

[33] T. Bruna-Larenas, J.S. Gómez-Jeria, A DFT and Semiempirical Model-Based Study of Opioid Receptor Affinity and Selectivity in a Group of Molecules with a Morphine Structural Core, *Int. J. Med. Chem.*, (2012) 16.

[34] J.S. Gómez-Jeria, P. Castro-Latorre, A Density Functional Theory analysis of the relationships between the Badger index measuring carcinogenicity and the electronic structure of a series of substituted Benz[a]anthracene derivatives, with a suggestion for a modified carcinogenicity index, *Chem. Res. J.*, 2 (2017) 112–126.

[35] J.S. Gómez Jeria, R. Ovando-Guerrero, A DFT Study of the Relationships between Electronic Structure and Central Benzodiazepine Receptor Affinity in a group of Imidazo[1,5-a]quinoline derivatives and a group of 3-Substituted 6-Phenyl-4H-imidazo[1,5-a]-[1,4]benzodiazepines and related compounds, *Chem. Res. J.*, 2 (2017) 170–181.

[36] A.G. Kpotin, G.S. Atohoun, A.U. Kuevi, A. Houngue-Kpota, J.-B. Mensah, J. Gómez Jeria, A quantum-chemical study of the relationships between electronic structure and anti- HIV-1 activity of a series of HEPT derivatives, *J. Chem. Pharm. Res.*, 8 (2016) 1019–1026.

[37] G. Kpotin, S.Y.G. Atohoun, A.U. Kuevi, A. Kpota-Hounguè, J.-B. Mensah, J.S. Gómez Jeria, A Quantum-Chemical study of the Relationships between Electronic Structure and Trypanocidal Activity against Trypanosoma Brucei Brucei of a series of Thiosemicarbazone derivatives, *Pharm. Lett.*, 8 (2016) 215–222.

[38] J.S. Gómez-Jeria, C. Moreno-Rojas, Dissecting the drug-receptor interaction with the Klopman-Peradejordi-Gómez (KPG) method I The interaction of 2,5-dimethoxyphenethylamines and their N-2-methoxybenzyl-substituted analogs with 5-HT1A serotonin receptors, *Chem. Res. J.*, 2 (2017) 27–41.

[39] A.G. Kpotin, G. Kankinou, U. Kuevi, J.S. Gómez Jeria, J.-B. Mensah, A Theoretical Study of the Relationships between Electronic Structure and Inhibitory Effects of Caffeine Derivatives on Neoplastic Transformation, *Int. Res. J. Pure Appl. Chem.*, 14 (2017) 1–10.

[40] J.S. Gómez-Jeria, S. Abarca-Martínez, A theoretical approach to the cytotoxicity of a series of β-carbolinedithiocarbamate derivatives against prostatic cancer (DU-145), breast cancer (MCF-7), human lung adenocarcinoma (A549) and cervical cancer (HeLa) cell lines, *Pharma Chem.*, 8 (2016) 507–526.

[41] M.J. Frisch, G.W. Trucks, H.B. Schlegel, G.E. Scuseria, M.A. Robb, J.R. Cheeseman, J.J.A. Montgomery, T. Vreven, S.S. Iyengar, J. Tomasi, V. Barone, B. Mennucci, M. Cossi, G. Scalmani, N. Rega, G03 Rev E01, Gaussian:, Pittsburgh, PA, USA, 2007.

[42] J.S. Gómez Jeria, D-Cent-QSAR: A program to generate Local Atomic Reactivity Indices from Gaussian 03 log files 10, Santiago de Chile, 2014.

[43] J.S. Gómez-Jeria, An empirical way to correct some drawbacks of Mulliken Population Analysis (Erratum in: J Chil Chem Soc, 55, 4, IX, 2010), *J. Chil. Chem. Soc.*, 54 (2009) 482–485.

[44] J.S. Gómez Jeria, Tables of proposed values for the Orientational Parameter of the Substituent II, *Res. J. Pharm. Biol. Chem. Sci.*, 7 (2016) 2258–2260.

[45] J.S. Gómez Jeria, Tables of proposed values for the Orientational Parameter of the Substituent I Monoatomic, Diatomic, Triatomic, n-C_nH_{2n}+1, O-n-C_nH_{2n}+1, NRR', and Cycloalkanes (with a single ring) substituents, *Res. J. Pharm. Biol. Chem. Sci.*, 7 (2016) 288–294.

[46] Statsoft, Statistica 80, 2300 East 14 th St. Tulsa, OK 74104, USA, 1984.

(Received 14 October 2017; accepted 02 November 2017)